CHAPTER 4

RESULT AND DISCCUSION

4.1 Preliminary Tests on Stainless Steel Channels

Before assembling, stainless steel flow flied plate is adequately cleared and clipped with two hydrophilic glasses. The end of channels is connected with stainless steel meshes to absorb water into the recycling tank. The main goal is to observe the capillary transport phenomenon for water. In this test, there are two holes (Fig. 4-1) on the top of stainless steel plate, one is air inlet and the other is water inlet.

In the preliminary tests, an interesting phenomenon can be observed after water and air are injected into the plate. The air convective force and the capillarity of multi-channels compel the water film to move forward (Fig. 4-1). With the air flow rate adjusted to 80, 60, 40, 20, 10, 5, 4, 2, and 1 ml/min, the water film still can be removed from the multi-channels, although the air flow rate becomes smaller. While water is injected into the surface of inlet section, it is sucked into channels rapidly and enters the stainless steel mesh by the capillary force. The mesh pumps out the excessive water from the multi-channels.

The above experiment indicates that the multi-channels in our design can handle the excessive water even with low air flow rate. It is worth noting that, with this design, one can solve flooding problem of DMFC effectively.

4.2 Integration of Single DMFC

4.2.1 In-situ Visualization of Cathode side of DMFC

The integrated single fuel cell is shown Fig. 4-2. The visualization experiments are operated under the following conditions. The methanol concentration is 2M, the methanol flow rate is 2 ml/min, the air flow rate is 80ml/min, and the operating temperature is 60℃. A CCD camera is employed to record the process of vapor condensation and water transport in the channels.

Methanol and air are injected into the integral DMFC continuously. In about 20 minutes, the operation becomes steady. The dynamic process of liquid water in the cathode channels is shown in Fig. 4-3. When the air flows through GDL surface, the vapor appears at GDL surface. In the beginning, some fog can be seen on the glass surface but gradually disappear with the temperature rise of the glass. Vapor contacts with hydrophilic glasses and condenses into droplet of water. It is noted that water condensation appears in the middle and rear part of the channels. Glass of the front part is clear, because the inlet air blows the vapor downstream.

As the DMFC works on, the condensed water accumulates continuously. A lot of small water drops appear on the glass surface, as shown in Fig. 4-4. In fact, water drops also form on the channel rib walls, as depicted in Fig. 4-5a. The drops keep growing and sometimes coalesce to form bigger drops. The drops on the walls slip downward due to gravity. There are cracks between the walls and the hydrophilic glass because the stainless steel plate is rough and uneven in surface.

Therefore, a part of drops exist in the cracks. First, the condensed water is full of the cracks to form long water film. Later, water films are like antennas on the walls and the hydrophilic glass. As the drops touch with the channel corners, they will be drained into the water film having formed therein and disappear rapidly, as shown in Fig. 4-5b. The water collected in the channel corners is transported downstream and absorbed by stainless steel mesh attached at the rear ends of the parallel. The water absorbed by the mesh will be stored in the water-storage tank.

The water transport behavior is shown in Fig. 4-6. It is observed that water exists in the corners and water films appear in the middle section of the flow channels. The dynamic water transport process is reflected by the oscillating motion of the water films.

Fig. 4-7 shows the flow field with gold-plated surface. The gold layer is used to improve the surface hydrophilicity and electrical conductivity of the stainless steel plate. It is expected that the condensed water on the gold-plated rib wall surface can spread effectively and be collected into the channel corners. The operation conditions are the same as those for the above experiment with uncoated stainless steel flow field plate. Again, the methanol concentration is 2M, the methanol flow rate is 2 ml/min, the air flow rate is 80ml/min, and the operating temperature is 60℃. Capillary force is stronger on hydrophilic surface. The contact angles of stainless steel, hydrophilic glass, and gold are about 60˚, 25˚, and 15˚, individually. The water transport process appears similarly, except that the water film on the gold-plated surface is thinner than on the stainless steel surface (Fig. 4-8). The gold surface with better hydrophilicity can spread the water films on the walls.

4.2.2 Performance Tests of DMFC

Several representative I-V curves of the cell with different operating conditions are shown in the following. The cell is placed in the constant-temperature oven for regulated operating temperatures, i.e., room temperature, 40℃, 60℃. The methanol concentration is 2M; the methanol flow rate is 2 ml/min, and the air flow rate is 80ml/min. It can be seen that current density increases with cell temperature, as expected, since both methanol oxidation kinetics and cathode kinetics improve with increasing temperature.

Fig. 4-9 shows the performances of stainless steel plate and gold-plated stainless steel plate with different temperatures. The maximum current and power output of stainless steel plate is 68.3mA/cm^2 at 0.016V and 7.26mW/cm^2 at 0.272V, respectively. The maximum current and power output of gold-plated stainless steel plate is 95mA/cm^2 at 0.016V and 13.2mW/cm^2 at 0.272V, respectively. The performance of gold-plated stainless steel is better as a result of better electrical conductivity and surface hydrophilicity.

Fig. 4-10 shows the polarization curves of stainless steel plate and gold-plated stainless steel plate with different air flow rates at 60℃. The performances both of stainless steel and gold-plated plate increase with air flow rate. According to this design, even if air flow rate is very low (10ml/min), air can be distributed uniformly on GDL. Therefore, the cell can operate smoothly with lower air rate (10ml/min).

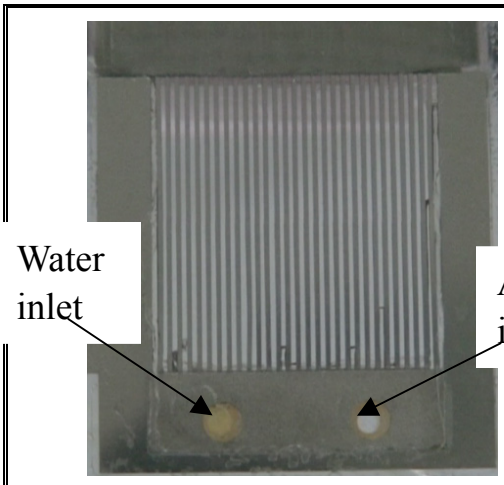	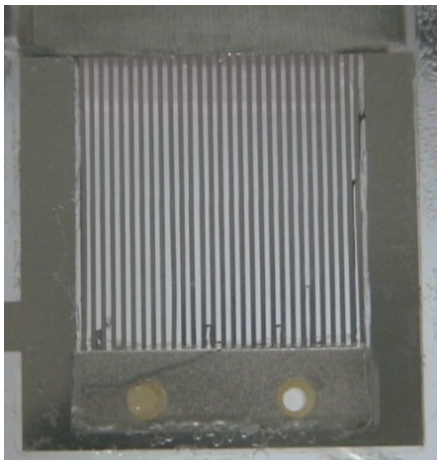
0s	3s
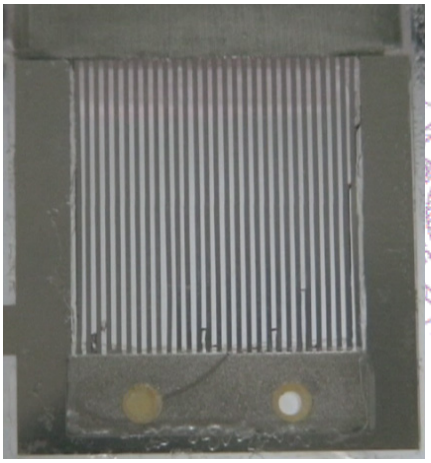	
6s	9s
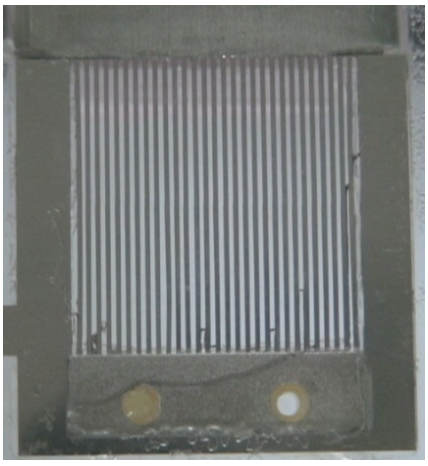	
12s	15s

Fig. 4-1 Dynamic process of SS flow flied plate with two hydrophilic glasses.

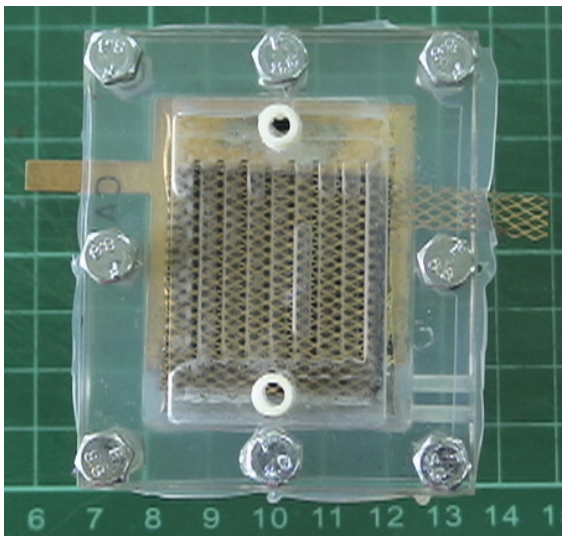

anode

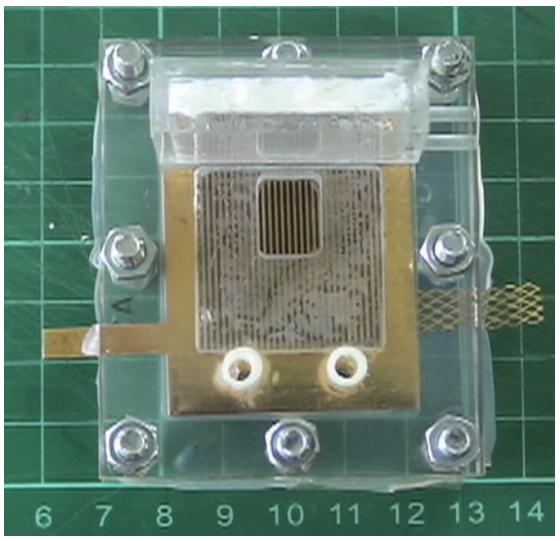

cathode

Fig. 4-2 Schematic of the integration of single fuel cell

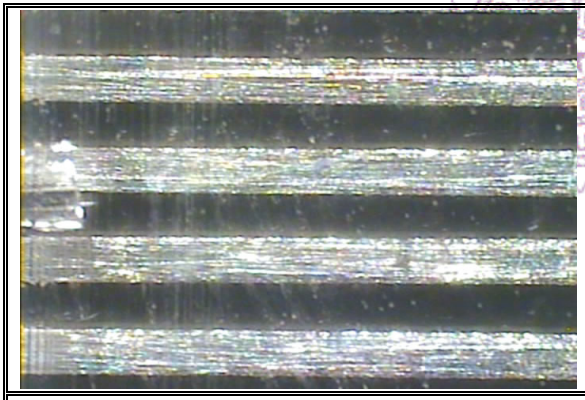

0s

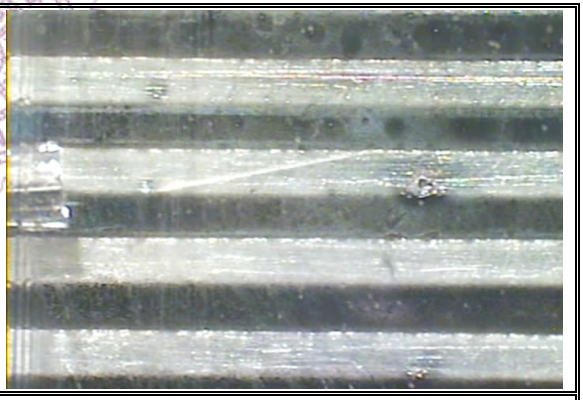

5s

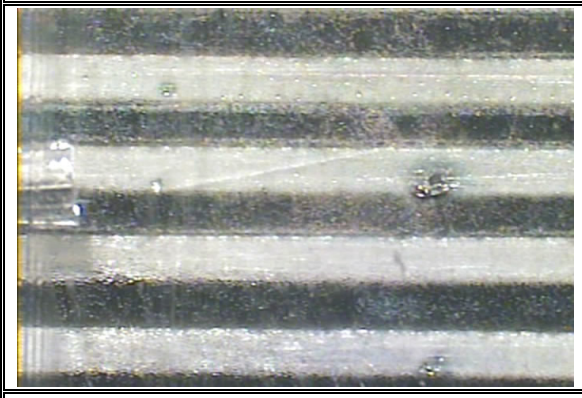

10s

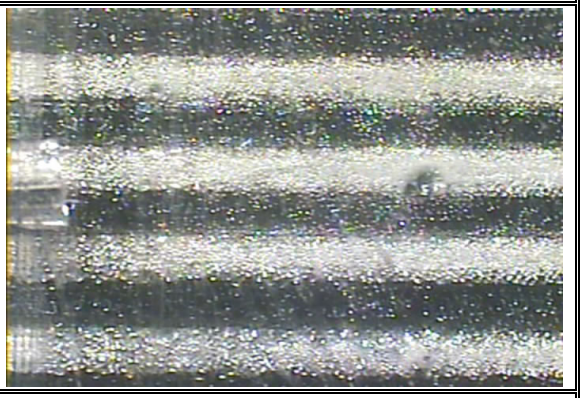

15s

Fig. 4-3 Schematic of vapor condensation on hydrophilic glasses in multi-channels

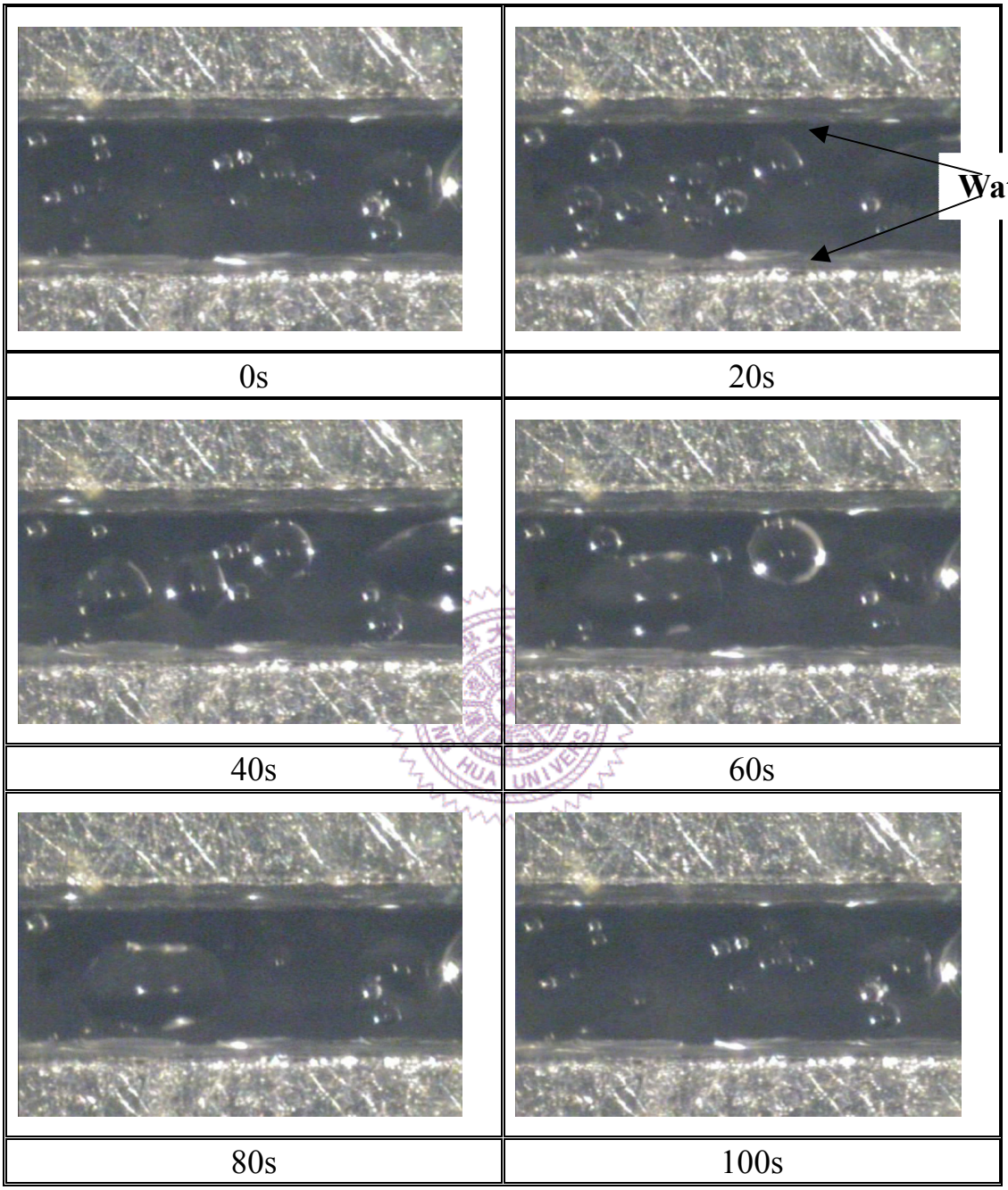

Fig. 4-4 Dynamic process of water droplets in a gas channel and accumulations of droplet on hydrophilic glasses

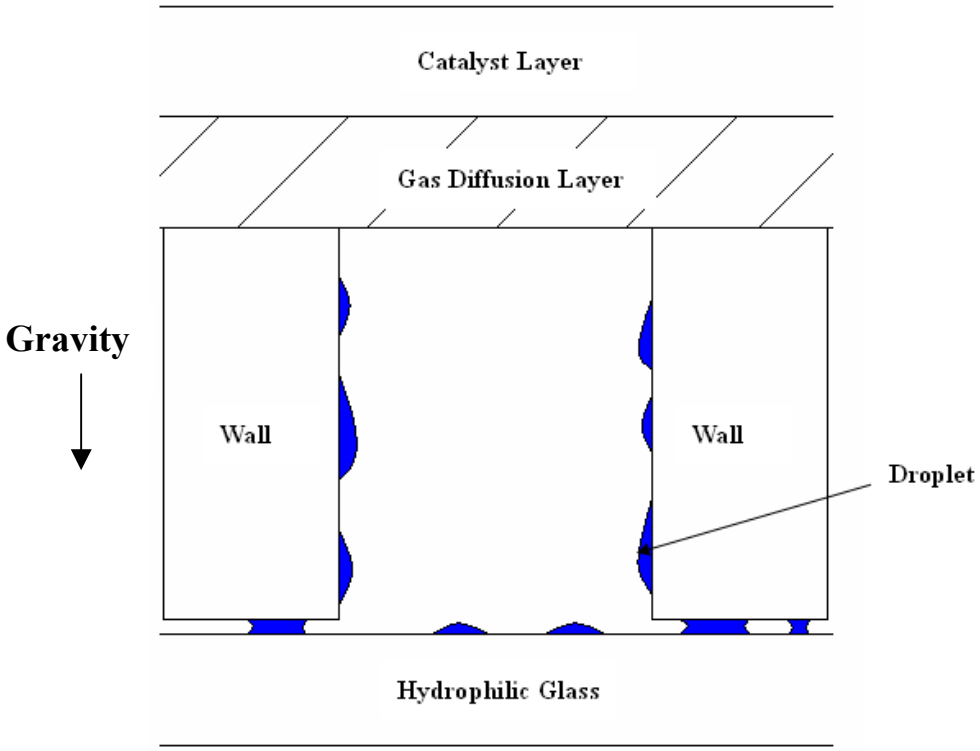

Fig. 4-5a Schematic of formation of the droplets

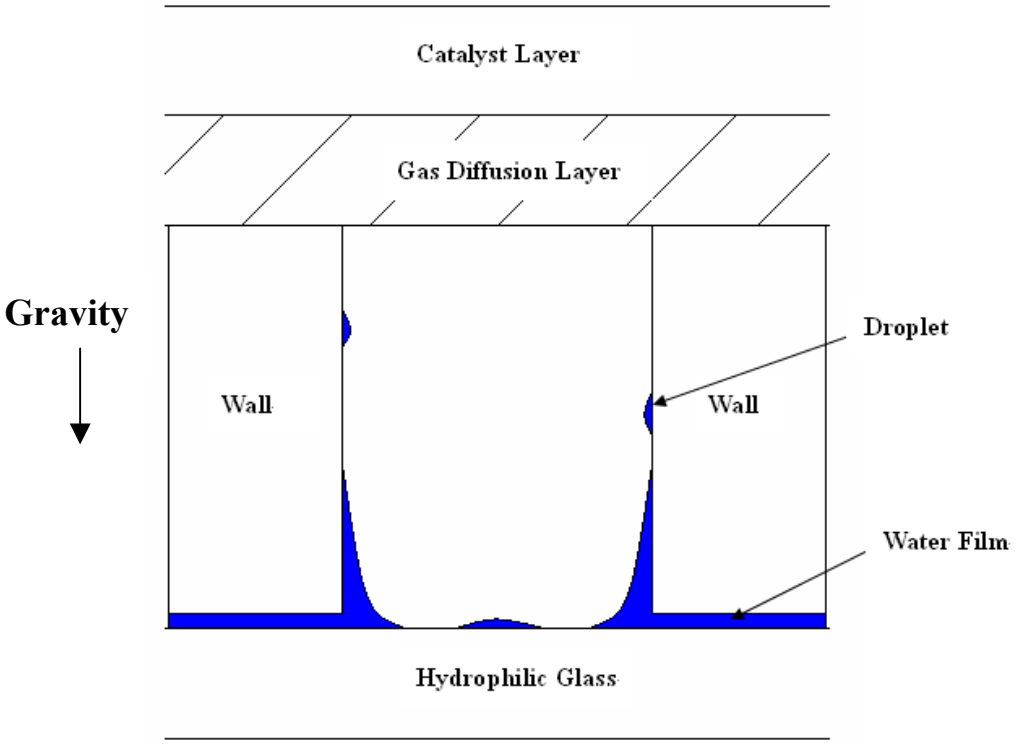

Fig. 4-5b Schematic of water film formation

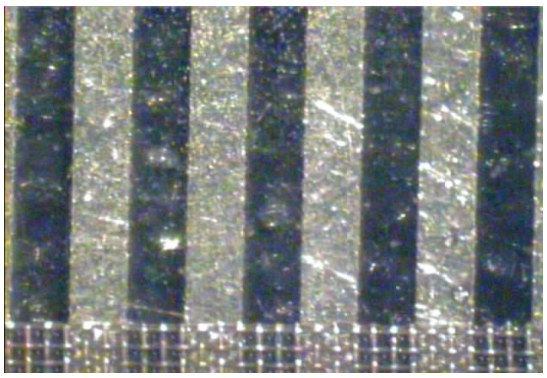

0S

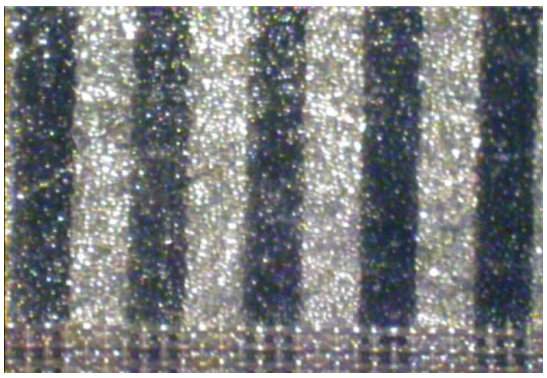

20S

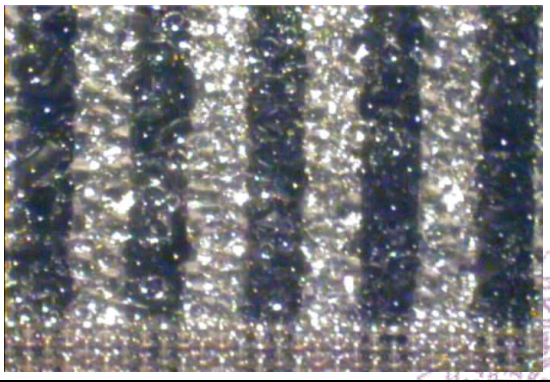

40s

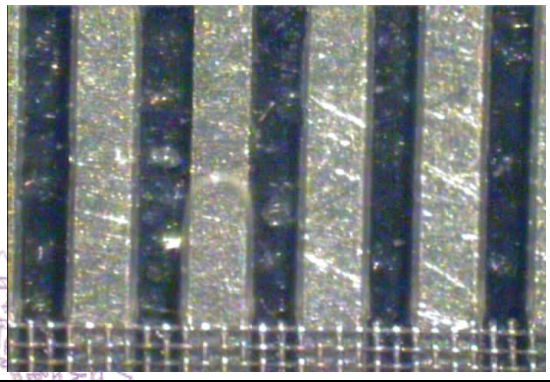

60S

Fig. 4-6 shows the water condensation process with gold-plated surface

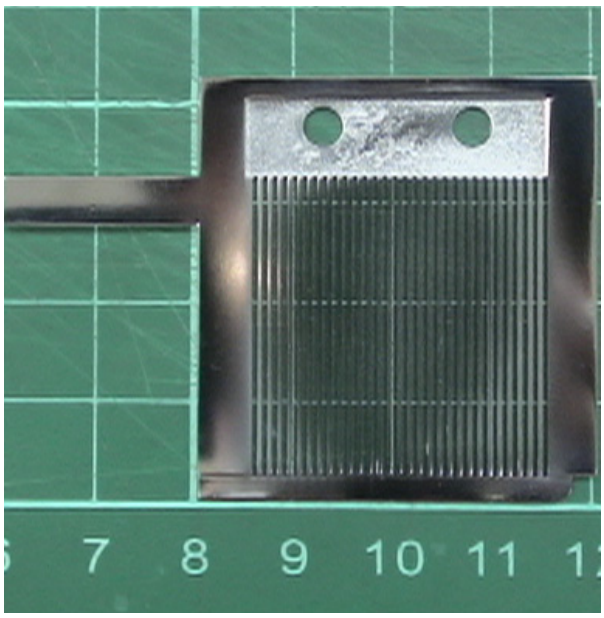

stainless steel plate

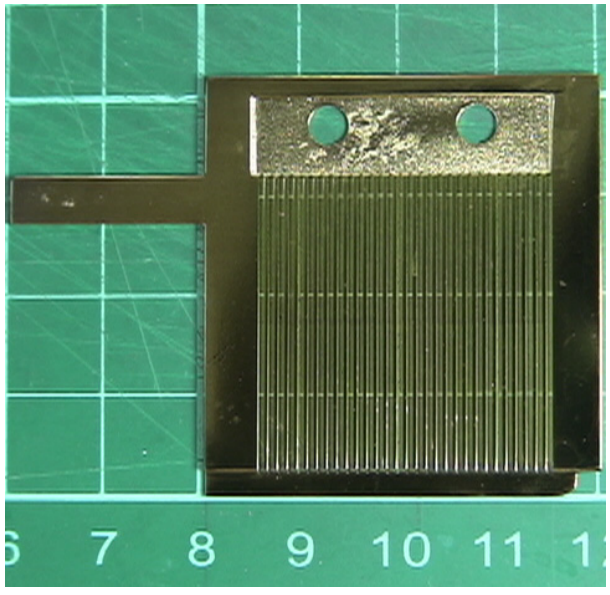

gold-plated stainless steel plate

Fig. 4-7 Schematic of the flow field with gold-plated surface

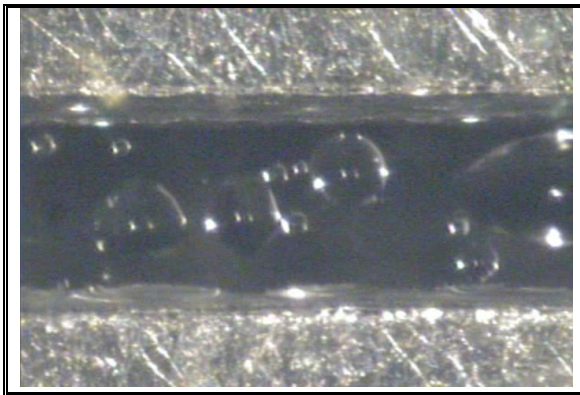

stainless steel channels

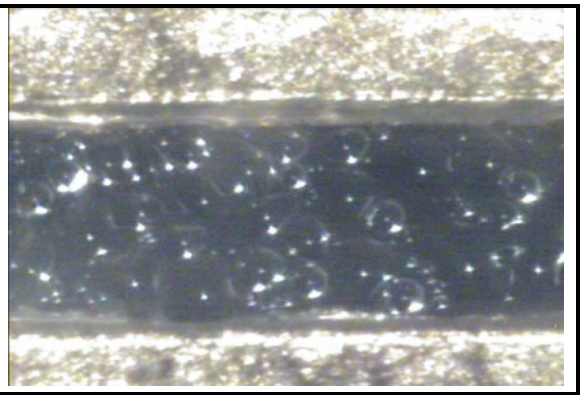

gold-plated stainless steel channels

Fig. 4-8 Comparison of stainless steel channels and gold-plated stainless steel channels

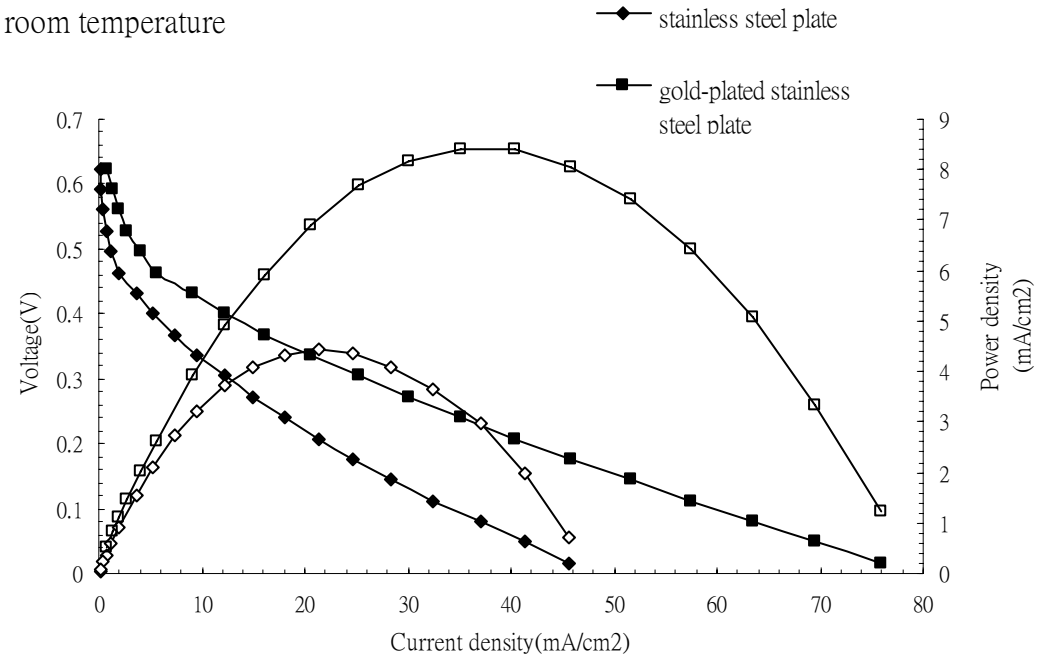

Fig. 4-9a Polarization curves of stainless steel plate and gold-plated stainless steel plate with room temperature

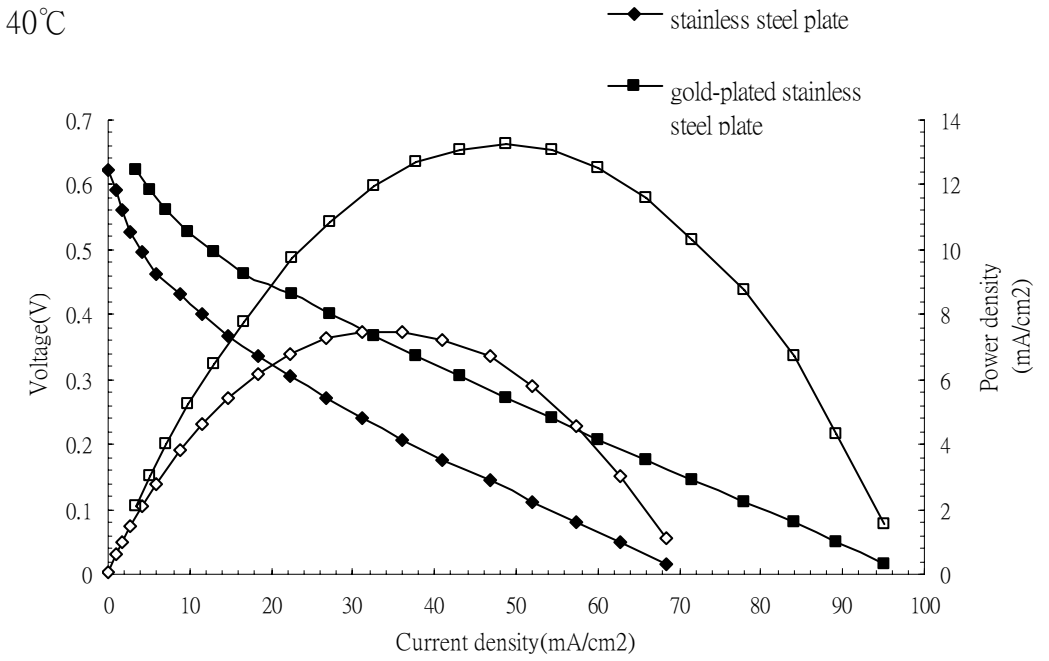

Fig. 4-9b Polarization curves of stainless steel plate and gold-plated stainless steel plate with 40℃

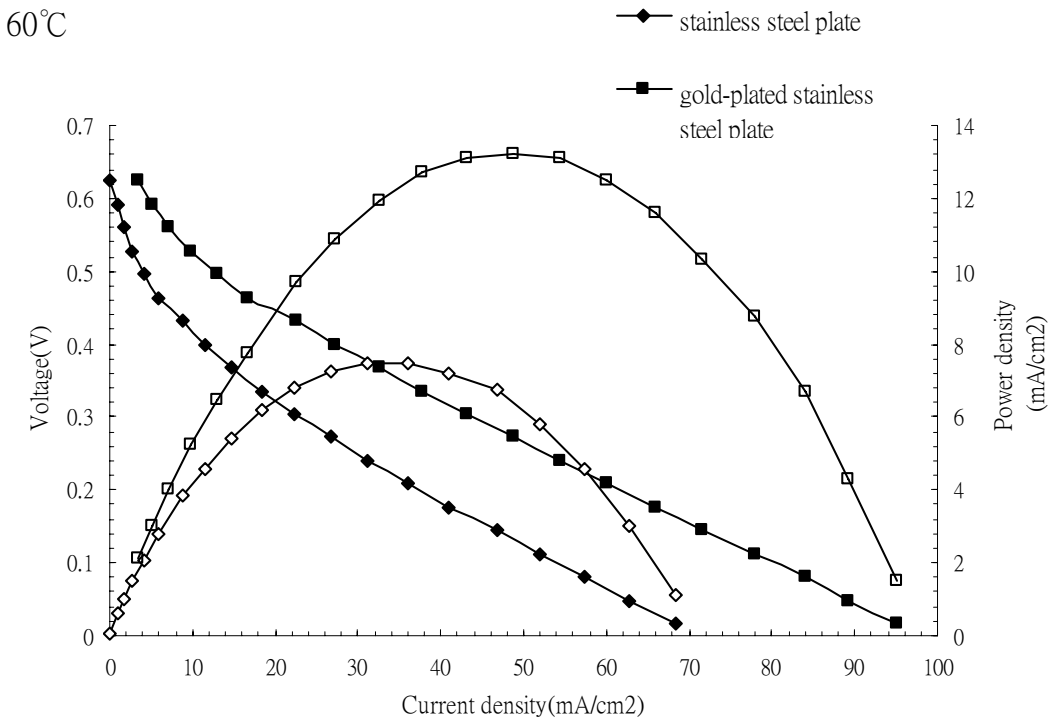

Fig. 4-9c Polarization curves of stainless steel plate and gold-plated stainless steel plate with 60℃

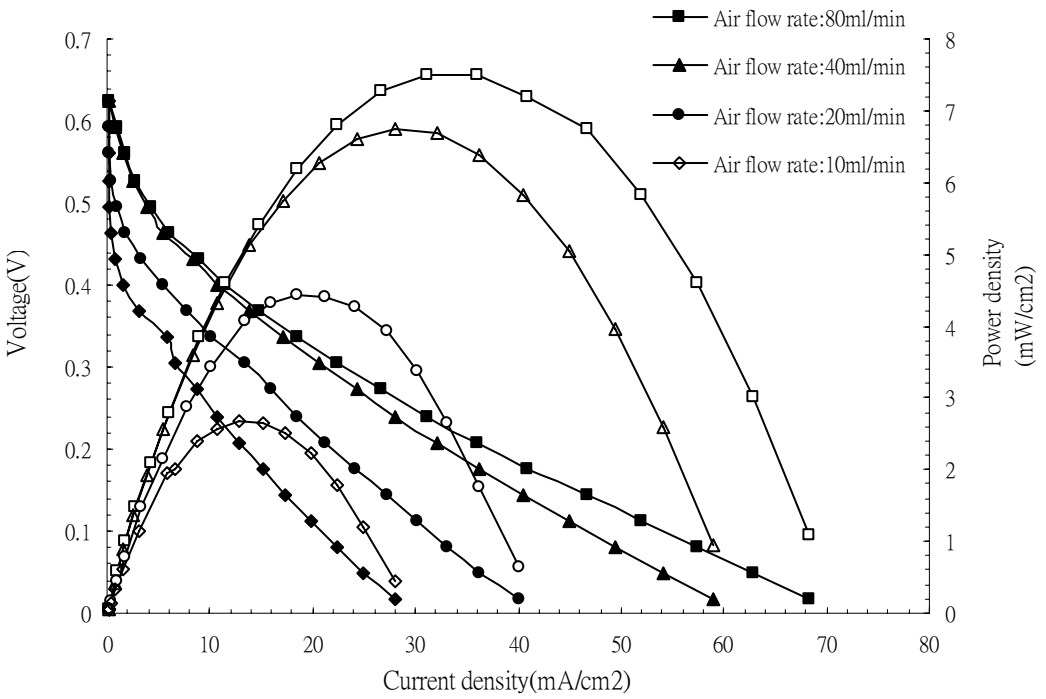

Fig. 4-10a Polarization curves of stainless steel plate with different air flow rates at 60℃

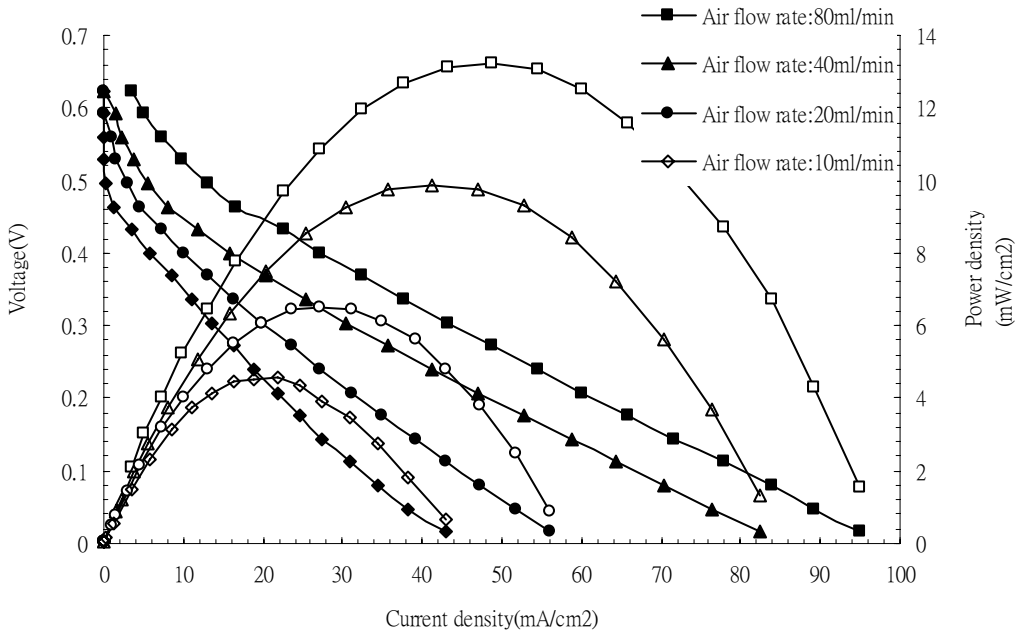

Fig. 4-10b Polarization curves of gold-plated stainless steel plate with different air flow rates at 60℃